ISSN 0021-3640, JETP Letters, 2006, Vol. 84, No. 9, pp. 518–523. © Pleiades Publishing, Inc., 2006.
Original Russian Text © I.S. Lyubutin, A.G. Gavriliuk, V.V. Struzhkin, S.G. Ovchinnikov, S.A. Kharlamova, L.N. Bezmaternykh, M. Hu, P. Chow, 2006, published in Pis'ma v Zhurnal Éksperimental'noĭ i Teoreticheskoĭ Fiziki, 2006, Vol. 84, No. 9, pp. 610–615.

Pressure-Induced Electron Spin Transition in the Paramagnetic Phase of the $GdFe_3(BO_3)_4$ Heisenberg Magnet

I. S. Lyubutin[a], A. G. Gavriliuk[a, b, c], V. V. Struzhkin[c], S. G. Ovchinnikov[d], S. A. Kharlamova[d, e], L. N. Bezmaternykh[d], M. Hu[e], and P. Chow[e]

[a] *Shubnikov Institute of Crystallography, Russian Academy of Sciences, Moscow, 119333 Russia*
e-mail: lyubutin@ns.crys.ras.ru
[b] *Institute of High-Pressure Physics, Russian Academy of Sciences, Troitsk, Moscow region, 142190 Russia*
[c] *Geophysical Laboratory, Carnegie Institution of Washington, Washington, DC 20015, USA*
[d] *Kirenskii Institute of Physics, Siberian Division, Russian Academy of Sciences, Akademgorodok, Krasnoyarsk, 660036 Russia*
[e] *Advanced Photon Source, ANL, Argonne, IL 60439, USA*

Received October 2, 2006

The HS ⟶ LS spin crossover effect (high-spin ⟶ low-spin transition) induced by high pressure in the range 45–53 GPa is observed in trivalent Fe^{3+} ions in the paramagnetic phase of a $Gd^{57}Fe_3(BO_3)_4$ gadolinium iron borate crystal. This effect is studied in high-pressure diamond-anvil cells by two experimental methods using synchrotron radiation: nuclear resonant forward scattering (NFS) and Fe K_β high-resolution x-ray emission spectroscopy (XES). The manifestation of the crossover in the paramagnetic phase, which has no order parameter to distinguish between the HS and LS states, correlates with the optical-gap jump and with the insulator–semiconductor transition in the crystal. Based on a theoretical many-electron model, an explanation of this effect at high pressures is proposed.

PACS numbers: 61.50.Ks, 71.27.+a, 71.30.+h, 81.40.Tv

DOI: 10.1134/S0021364006210119

1. INTRODUCTION

The $GdFe_3(BO_3)_4$ crystal possesses a trigonal symmetry with the space group $R32$ (D_{3h}^7) [1]. The structure consists of layers composed of trigonal GdO_6 prisms and smaller size FeO_6 octahedra, which form helicoidal one-dimensional chains weakly bonded with each other and extended along the c axis [1]. $GdFe_3(BO_3)_4$ is an antiferromagnet with the Neel point $T_N = 38$ K, and a spin reorientation transition (spin flop) occurs in the crystal at about 10 K [2, 3]. It is suggested that, below T_N, magnetic ordering relates to iron ions, while Gd^{3+} ions, remaining paramagnetic, are magnetized by the iron sublattice and markedly affect the anisotropic properties of the crystal [2–5]. A magnetoelectric effect has recently been detected in this crystal, because of which this material can be assigned to multiferroics [6]. Electric polarization and magnetostriction arise in $GdFe_3(BO_3)_4$ at low temperatures as a result of a change in magnetic symmetry because of spin reorientation induced by an applied magnetic field. Upon exposure to high pressures, structural and electronic phase transitions were revealed in a $GdFe_3(BO_3)_4$ crystal in the region of $P = 26$ and 43 GPa with a stepwise decrease in the optical gap and an insulator–semiconductor transition [7, 8].

Thus, external actions lead to new effects and strongly affect the properties of $GdFe_3(BO_3)_4$. In this work, the spin crossover effect associated with the transition of Fe^{3+} ions from the high-spin (HS) to low-spin (LS) state has been revealed upon exposure to high pressures created in diamond-anvil cells. This effect has been studied by two independent experimental methods using synchrotron radiation: nuclear resonant forward scattering (NFS) and Fe K_β high-resolution x-ray emission spectroscopy (XES).

2. METHODS AND EXPERIMENTAL RESULTS

$GdFe_3(BO_3)_4$ single crystals were grown from a solution in a melt [9]. Crystals with the ^{57}Fe isotope (enrichment up to 96%) were grown by a specially elaborated procedure for nuclear resonant investigations. The x-ray diffraction patterns for the reference and isotopically enriched $GdFe_3(BO_3)_4$ samples indicated that the phase and structural compositions of these crystals are identical.

We used diamond-anvil cells (DACs) for measurements at high pressures. The diameter of the working area of diamonds was about 300 μm, and the diameter of the hole in the gasket in which the sample was placed was about 100 μm. A beryllium gasket was used in XES

experiments, and a rhenium foil was used in the measurements of NFS spectra and in x-ray diffraction experiments. Helium, which is the most hydrostatic medium, was used as the pressure medium in XES experiments, and argon was used in x-ray diffraction and NFS experiments. The pressure and its possible gradients with respect to the diameter of the sample were measured by the shift of the ruby fluorescence line. For this purpose, several pieces of ruby about 1 μm in size were placed in the cell besides the sample; these pieces were placed at different distances from the center in order to estimate the pressure gradient.

From Mossbauer spectroscopy data, it was found that the absorption spectrum from ^{57}Fe nuclei of the $GdFe_3(BO_3)_4$ crystal consisted of one doublet with the quadrupole splitting $QS = 0.287(2)$ mm/s and the isomeric shift $IS = 0.385(2)$ mm/s (in reference to metallic iron). These parameters indicate that Fe^{3+} ions are in the high-spin state under normal conditions.

2.1. Experiments on the Nuclear Resonant Forward Scattering of Synchrotron Radiation (SR)

A $Gd^{57}Fe_3(BO_3)_4$ crystal enriched with the Fe-57 isotope was used for synchrotron Mossbauer experiments (nuclear forward scattering, NFS) at high pressures. To obtain a thin sample, the crystal was ground to powder, and a plate ~3.8-μm thick was prepared from the powder by preliminarily pressing the powder between diamond anvils. In an optical microscope, the plate was transparent and almost colorless. The plate $\sim 80 \times 80$ μm^2 in size was placed in the working volume of the DAC, which was filled with argon (the pressure medium).

NFS experiments were performed on the beamline 16-ID-D research synchrotron station in Argonne (APS, Argonne, United States). A 24-bunch operation mode was used at which pulses of the SR beam were separated with a time interval of 154 ns. Resonant forward scattering spectra from ^{57}Fe nuclei (time or synchrotron Mossbauer spectra [10]) were recorded at room temperature upon the pressure increase up to $P =$ 58.3 GPa.

The evolution of NFS spectra with increasing pressure is shown in Fig. 1. The damped decay of nuclear excitation is modulated over time with quantum and dynamic beats. Quantum beats arise upon splitting the nuclear levels by hyperfine interactions into sublevels due to interference between scattered radiation components of differing frequencies. Because the $GdFe_3(BO_3)_4$ crystal at room temperature occurs in a paramagnetic state, quantum beats of the magnetic nature are absent, and the observed beats are due to the electric quadrupole hyperfine splitting of the excited level of a ^{57}Fe nucleus (nuclear spin $I = \pm 3/2$) into two sublevels. The period of quantum beats is inversely proportional to the hyperfine splitting. Dynamic beats are due to multiple scattering processes in the "thick" crystal and are determined by the thickness of the sample [11]. In the case when the period of quantum beats is close to the time interval between the SR bunches, taking into account dynamic beats is extremely important for the correct evaluation of hyperfine parameters from the NFS data, and as thin samples as possible should be used to minimize the effect of dynamic beats [12].

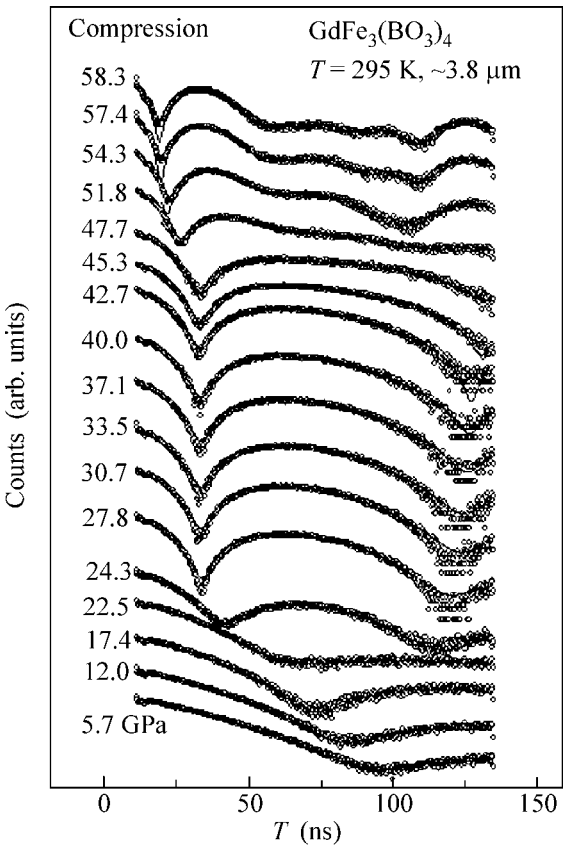

Fig. 1. Evolution of NFS spectra (points) with increasing pressure in the $GdFe_3(BO_3)_4$ crystal enriched with the ^{57}Fe isotope (at room temperature). The pressure-transferring medium in the DAC is argon. Lines are the calculated spectra approximated by the MOTIF program; ○ are experimental points.

Experimental NFS spectra were processed by the MOTIF program [13], and calculated spectra are presented in Fig. 1 in solid lines. It follows from experiment that three regions exist in the studied range of pressures in which the $GdFe_3(BO_3)_4$ crystal occurs in different phase states. These regions are separated by two phase transitions, the first of which occurs at a pressure of about 25 GPa, and the second one occurs in the region ~45–53 GPa.

The pressure dependence of the quadrupole splitting QS obtained from the NFS spectra is shown in Fig. 2a. A small increase in QS is observed in the low-pressure phase $0 < P < 25$ GPa with increasing P, and then a sharp jump of QS to a value of ~1.0 mm/s occurs at $P =$ 25 GPa. This is evidently associated with a structural

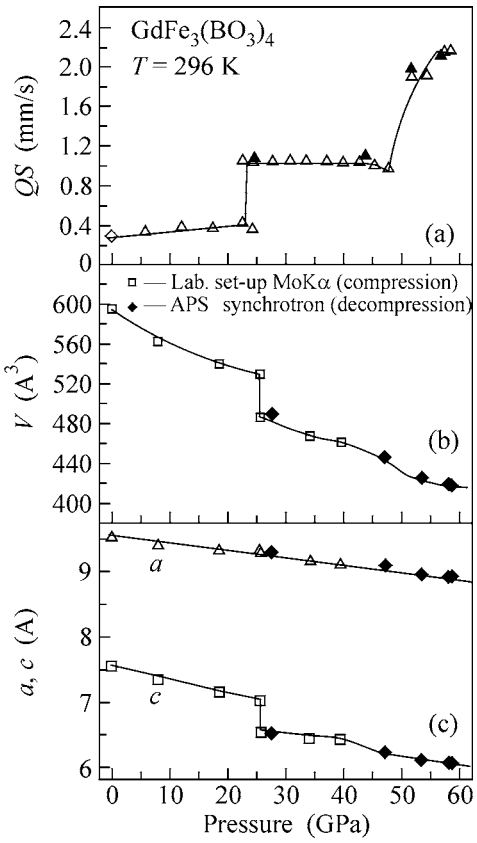

Fig. 2. (a) Pressure dependence of the quadrupole splitting *QS* in the $Gd^{57}Fe_3(BO_3)_4$ crystal obtained from the NFS spectra and (b and c) variation of the unit cell volume (*V*) and parameters (*a* and *c*) from two series of measurements: with increasing pressure (light points, laboratory Mo K_α source) and with decreasing pressure (dark points, synchrotron APS source).

phase transition at which the collapse of the unit cell volume by 8% was detected [7]. The significant increase in *QS* due to the lattice contribution points to distortions of oxygen octahedra in the environment of Fe^{3+} ions arising in this transition. The value of *QS* remains constant in the intermediate phase $25 < P < 45$ GPa, and the second transition and a new increase in *QS* starts at $P > 45$ GPa (see Fig. 2a). This transition spreads over approximately 8 GPa, and the value of *QS* reaches a very high value of ≈2.2 mm/s at its end in the high-pressure phase. This is indicative of a change in the electron spin structure of iron ions. A significant increase in the electric field gradient at an iron nucleus occurs because of the appearance of a large electronic contribution to *QS* due to the violation of the spherical symmetry of the electronic shell of Fe^{3+} upon transition from the high-spin to low-spin state. Thus, the second transition is associated with the spin HS ⟶ LS (high-spin ⟶ low-spin) crossover.

We also measured several NFS spectra in the pressure-decreasing mode. It was found that the spin crossover effect is reversible (see dark triangles in Fig. 2a); that is, the HS state restores below the critical pressure.

2.2. X-ray Diffraction

To study possible changes in the crystal structure upon spin HS–LS crossover, x-ray diffraction patterns were also measured simultaneously with the NFS spectra in the same DAC in the pressure-decreasing mode. It was found that the x-ray diffraction patterns before and after the HS–LS transition correspond to the same symmetry of the crystal. Previously, we found that the jump in the unit cell volume at ~26 GPa also occurs without a change in the symmetry of the $GdFe_3(BO_3)_4$ crystal [7]. Thus, the symmetry of the $GdFe_3(BO_3)_4$ crystal is conserved in the entire range of pressures $0 < P < 60$ GPa, in spite of a number of transformations such as the insulator–semiconductor transition [7] and spin crossover.

The variation of the unit cell volume and parameters of the $GdFe_3(BO_3)_4$ crystal from two series of our measurements (in the range of pressures $0 < P < 60$ GPa) is shown in Figs. 2b and 2c. It is seen that only a slightly pronounced anomaly is observed in the region of spin crossover 45–53 GPa. This is an additional proof that the sharp increase in the quadrupole-splitting parameter *QS* in this region is not associated with a change in the crystal structure and is rather due to an electronic transition.

2.3. Fe K_β High-Resolution X-ray Emission Spectroscopy

The spin crossover effect can also be studied using the high-resolution x-ray emission spectroscopy (XES) technique, which is sensitive to the spin state and electronic structure of iron ions [14, 15]. In the case of the high-spin state of iron, the x-ray emission spectrum of Fe is presented by the main intense $K_{\beta_{1,3}}$ peak with an energy of 7058 eV and a weakly intense satellite peak $K_{\beta'}$ with a lower energy (see Fig. 3). This satellite peak arises as a result of the exchange interaction of the inner 3*p* hole with 3*d* electrons at the final stage of the emission process. Because the spin in the low-spin LS state of the Fe^{3+} ion (d^5 configuration, spin $S = 1/2$) is five times lower than the spin in the high-spin HS state (spin $S = 5/2$), the collapse of the magnetic moment as a result of this transition is manifested as a sharp decrease in the intensity of the satellite peak [15]. However, because the intensity of x-ray emission spectra is low, reliable data can be obtained only using synchrotron radiation sources.

Our high-pressure studies of XES spectra on a $GdFe_3(BO_3)_4$ single crystal were performed on the beamline 16-ID-D research synchrotron station in Argonne (APS, Argonne, United States). The size of the single-crystal plate was 60 × 30 × 12 μm, which agrees well with the shape of the SR beam cross sec-

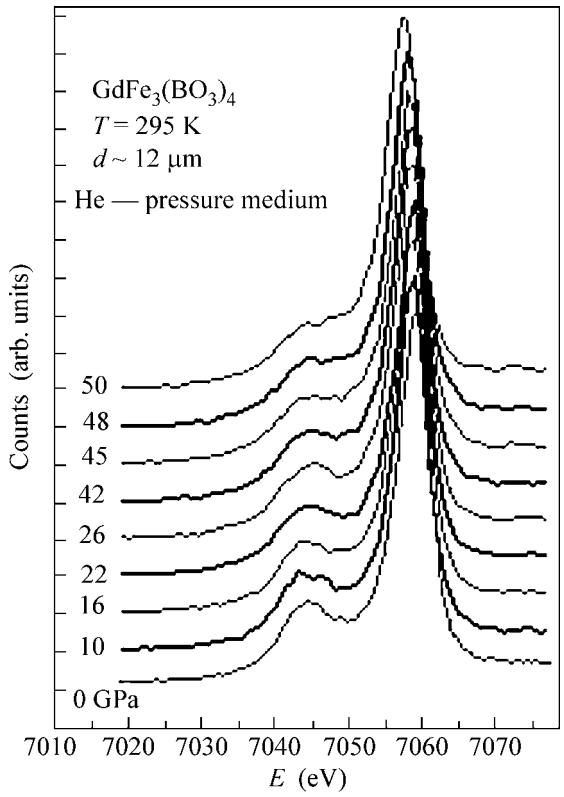

Fig. 3. Evolution of Fe K_β x-ray emission spectra in the $GdFe_3(BO_3)_4$ crystal with increasing pressure at room temperature. The pressure-transferring medium in the DAC is helium.

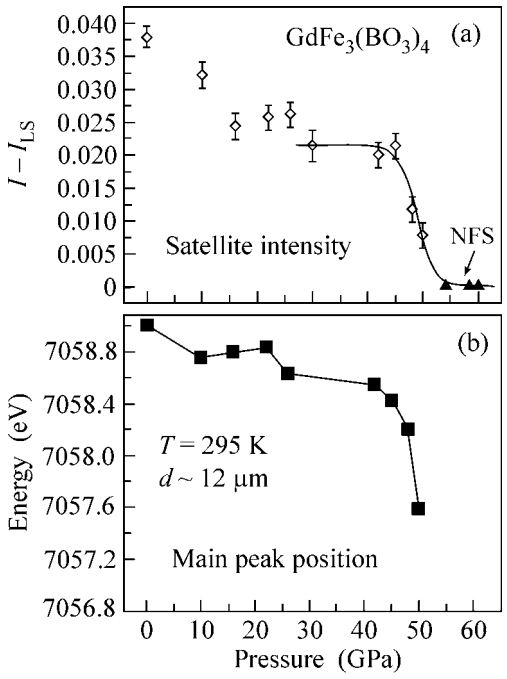

Fig. 4. Pressure dependence of (a) the parameter $R = [I(P) - I_{LS}]$ proportional to the relative population of the high-spin state in the $GdFe_3(BO_3)_4$ crystal. Solid line is the approximation of the XES experimental data in the spin crossover region by the calculated curve based on the model of thermal fluctuations (Eq. (1)); (b) the main peak position in Fe K_β x-ray emission spectra.

tion. The XES spectra were measured at room temperature in a DAC with a helium medium at high pressures of up to 52 GPa. The evolution of Fe K_β x-ray emission spectra with increasing pressure is shown in Fig. 3. Visually, the satellite peak intensity weakly varies in the pressure range $0 < P < 40$ GPa; however, it decreases rapidly above 40 GPa. The pressure dependence of the parameter $R = [I(P) - I_{LS}]$ is shown in the pressure-increasing mode in Fig. 4a. The parameter R equals the difference of the integral spectral intensities at the pressure P [$I(P)$] and at an above-critical pressure $P > P_C$ [I_{LS}], that is, in the low-spin state. This parameter reflects the relative population of the high-spin phase in the transition region. It is seen in Fig. 4a that the parameter R noticeably decreases with increasing pressure in the range $0 < P < 25$ GPa. The cause of this behavior is not yet clear and requires additional, more comprehensive experimental and theoretical investigations. The value of R above 25 GPa is virtually constant. At ~45 GPa, it starts to drop sharply and decreases to a zero value at 51 GPa, which corresponds to the complete transition to the low-spin state.

At $P > 40$ GPa, the position of the main peak sharply displaces by ~1 eV towards low energies (see Fig. 4b). This is also characteristic of the HS–LS transition [15]. Measurements show that the satellite peak intensity does not drop to zero after the transition. This agrees with the fact that the LS state of the Fe^{3+} ion is not diamagnetic (as it can be in the case of divalent iron) but has the spin $S = 1/2$. We found that the transition is not stepwise and has a width of about 6 GPa in an XES experiment. This significant broadening of the transition range cannot be explained by the pressure gradient, because helium as the pressure-transferring medium in the XES experiment is very soft, and the pressure inhomogeneity in a DAC does not exceed 0.5 GPa. The causes of this effect are discussed below.

3. DISCUSSION

The spin crossover phenomenon upon exposure to high pressures has recently been observed in a number of magnetic dielectrics such as $FeBO_3$ [16, 17], $BiFeO_3$ [18], (La, Pr)FeO_3 [19, 20], Fe_2O_3 [21], and $Y_3Fe_5O_{12}$ [22]. In all these cases, iron ions are in the trivalent state Fe^{3+} and the HS–LS spin crossover is manifested as the collapse of the local magnetic moment and as the transition of the antiferromagnet to a paramagnetic state. The peculiarity of these investigations is that the spin crossover in the $GdFe_3(BO_3)_4$ crystal occurs in the para-

magnetic phase, which has no order parameter to distinguish between the HS and LS states. The Neel point in this crystal at normal pressure is rather low (38 K) and cannot exceed room temperature as the pressure grows (see, e.g., [17]); therefore, our measurements were performed in the certainly paramagnetic phase.

3.1. Calculation of the Average Spin in the Vicinity of the Crossover and Comparison with Experiment

It is sufficient to consider two of the entire set of Fe^{3+} terms: the HS $^6A_1$ term with spin $S = 5/2$ and the energy $E_{5/2}$ and the LS $^2T_2$ term with spin $S = 1/2$ and the energy $E_{1/2}$. At zero pressure, $E_{5/2} < E_{1/2}$; however, with increasing pressure, the energy $E_{1/2}$ decreases faster than $E_{5/2}$ due to an increase in the crystal field parameter Δ, which leads to the crossover of these levels at $\Delta = \Delta_c$ [23]. The population numbers of terms with spin S can be written as

$$n_S = \exp(-E_S/kT)/Z, \quad (1)$$

where the statistical sum Z in the case of two terms equals

$$Z = \exp(-E_{5/2}/kT) + \exp(-E_{1/2}/kT). \quad (2)$$

As a result, we obtain for the average spin projection

$$\begin{aligned}\langle S^Z \rangle &= \frac{5}{2}n_{5/2}(P,T) + \frac{1}{2}n_{1/2}(P,T) \\ &= \left[\frac{5}{2} + \frac{1}{2}\exp(-\Delta E/kT)\right]/[1 + \exp(-\Delta E/kT)],\end{aligned} \quad (3)$$

where $n_{5/2}$ and $n_{1/2}$ are the probabilities of finding the Fe^{3+} ion in the state $S = 5/2$ and $S = 1/2$. At $T = 0$ K, the probability $n_{5/2}$ equals unity up to the crossover point and zero above P_{cr}.

The energy gap between terms equals $\Delta E(P) = E_{1/2} - E_{5/2} = 15B + 10C - 2\Delta$, where B and C are the Racah parameters. It is suggested that B and C weakly depend on the pressure, and Δ increases linearly with pressure $\Delta(P) = \Delta(0) + \alpha_\Delta P$ [24]. The value of α_Δ for the $FeBO_3$ borate crystal has recently been estimated at 0.018 eV/GPa from the behavior of the optical spectra under pressure [25], and $B = 0.084$ eV and $C = 0.39$ eV at a zero pressure [24].

When approximating experimental data with a theoretical curve, we use the fact that the above parameter $R = [I(P) - I_{LS}]$ reflects the relative population of the high-spin state n_S [see Eq. (1)] and depends on pressure and temperature in an analogous way. In the fitting, we took into account that $R_{LS} = 0$ and $kT = 0.025$ eV (room temperature). The results of this fitting are shown by a solid line in Fig. 4a. The fitting parameters were found to be $P_c = 48.78$ GPa and $\alpha_\Delta = 0.0077$ eV/GPa.

It is notable that the parameter α_Δ for the $GdFe_3(BO_3)_4$ crystal turned out to be two times smaller than that found for the $FeBO_3$ borate, which is evidently due to differences in the crystal structure and the compressibility of these compounds [7, 26].

3.2. Phase Transition or Crossover?

Above, we used the terms two phase transitions and electronic transitions at $P_1 = 25$ GPa and $P_2 = 45$ GPa. These terms need to be defined more accurately. The transition at P_1 from the low-pressure phase to the intermediate phase is accompanied by a structural phase transition of the first order. In this sense, it is a thermodynamic phase transition. The jump of the lattice parameter c and the unit cell volume at point P_1 (see Fig. 2) leads to a jump of the crystal field and, hence, to the jumps of the dielectric gap and the optical absorption edge observed in [7]. In this case, the electronic transition accompanies the structural one.

As to the spin crossover, its smearing at finite temperatures already indicates that this is not a genuine phase transition in the thermodynamic sense. It is seen from Eq. (3) that the smearing width decreases with decreasing temperature. At $T = 0$, the spin will change stepwise, and it would be possible to discuss the quantum phase transition by a parameter (pressure, in this case). However, as temperature decreases, magnetic ordering occurs in the $GdFe_3(BO_3)_4$ crystal and a magnetic order parameter appears. Transitions under pressure in $GdFe_3(BO_3)_4$ at low temperatures will evidently not differ from the magnetic collapse in $FeBO_3$ studied previously [16, 17]. The special feature of these investigations is that we observed the HS–LS crossover for Fe^{3+} ions in the paramagnetic region (at $T = 300$ K). For $FeBO_3$, the similar crossover could be observed at $T > 600$ K.

Note that a similar effect has recently been observed in the (Mg, Fe)O magnesiowüstite containing divalent Fe^{2+} ions [12], with the only difference that the HS–LS spin crossover leads to the state with the zero spin $S = 0$, and the crystal becomes diamagnetic. In this regard, it is very interesting and important for fundamental physics and geophysics to study experimentally the temperature dependence of the HS–LS transition width in such materials and to construct the P–T phase diagram of spin states.

ACKNOWLEDGMENTS

This work was supported by the Russian Foundation for Basic Research, project no. 05-02-16142-a; by the Program of the Division of Physical Science of the Russian Academy of Sciences on Strongly Correlated Electronic Systems; and by DOE, project no. DE-FG02-02ER45955. HPCAT is the form of collaboration between the Carnegie Institution, Lawrence Livermore National Laboratory, the University of Hawaii, the University of Nevada Las Vegas, and the Carnegie/DOE Alliance Center (CDAC) and is supported by DOE-

BES, DOE-NNSA, NSF, DOD-TACOM, and the W.M. Keck Foundation. The use of Advanced Photon Source is supported by the US Department of Energy, Basic Energy Science, Office of Science in the framework of contract no. W-31-109-EN.

REFERENCES

1. N. I. Leonyuk and L. I. Leonyuk, Prog. Cryst. Growth Charact. **31**, 179 (1995); N. I. Leonyuk, Prog. Cryst. Growth Charact. **31**, 279 (1995).
2. A. D. Balaev, L. N. Bezmaternykh, I. A. Gudim, et al., J. Magn. Magn. Mater. C **258–259**, 532 (2003).
3. S. A. Kharlamova, S. G. Ovchinnikov, A. D. Balaev, et al., Zh. Éksp. Teor. Fiz. **128**, 1252 (2005) [JETP **101**, 1098 (2005)].
4. A. I. Pankrats, G. A. Petrakovski, L. N. Bezmaternykh, et al., JETP **99**, 766 (2004).
5. A. K. Zvezdin, V. M. Matveev, A. A. Mukhin, and A. I. Popkov, *Rare-Earth Ions in the Magnetic Ordered Crystals* (Nauka, Moscow, 1985) [in Russian].
6. A. K. Zvezdin, S. S. Krotov, A. M. Kadomtseva, et al., JETP Lett. **81**, 335 (2005).
7. A. G. Gavrilyuk, S. A. Kharlamova, I. S. Lyubutin, et al., Pis'ma Zh. Éksp. Teor. Fiz. **80**, 482 (2004) [JETP Lett. **80**, 426 (2004)].
8. A. G. Gavriliuk, S. A. Kharlamova, I. S. Lyubutin, et al., J. Phys.: Condens. Matter. **17**, 7599 (2005).
9. L. N. Bezmaternykh, S. A. Kharlamova, and V. L. Temerov, Kristallografiya **49**, 945 (2004) [Crystallogr. Rep. **49**, 855 (2004)].
10. R. Ruffer and A. I. Chumakov, Hyperfine Interact. **97/98**, 589 (1996).
11. G. V. Smirnov, Hyperfine Interact. **123/124**, 31 (1999).
12. A. G. Gavriliuk, J.-F. Lin, I. S. Lyubutin, et al., JETP Lett. **84**, 190 (2006).
13. Yu. V. Shvyd'ko, Hyperfine Interact. **125**, 173 (2000).
14. J. Badro, G. Fiquet, V. V. Struzhkin, et al., Phys. Rev. Lett. **89**, 205504 (2002).
15. J. Badro, V. Struzhkin, J.-F. Shu, et al., Phys. Rev. Lett. **83**, 4101 (1999).
16. I. A. Troyan, A. G. Gavrilyuk, V. A. Sarkisyan, et al., Pis'ma Zh. Éksp. Teor. Fiz. **74**, 26 (2001) [JETP Lett. **74**, 24 (2001)].
17. A. G. Gavriliuk, I. A. Trojan, I. S. Lyubutin, et al., Zh. Éksp. Teor. Fiz. **127**, 780 (2005) [JETP **100**, 688 (2005)].
18. A. G. Gavriliuk, V. V. Struzhkin, I. S. Lyubutin, et al., Pis'ma Zh. Éksp. Teor. Fiz. **82**, 243 (2005) [JETP Lett. **82**, 224 (2005)].
19. G. R. Hearne, M. P. Pasternak, R. D. Taylor, et al., Phys. Rev. B **51**, 11 495 (1995).
20. W. M. Xu, O. Naaman, G. Kh. Rozenberg, et al., Phys. Rev. B **64**, 094411 (2001).
21. M. P. Pasternak, G. Kh. Rozenberg, G. Yu. Machavariani, et al., Phys. Rev. Lett. **82**, 4663 (1999).
22. I. S. Lyubutin, A. G. Gavrilyuk, I. A. Troyan, et al., Pis'ma Zh. Éksp. Teor. Fiz. **82**, 797 (2005) [JETP Lett. **82**, 702 (2005)].
23. V. N. Zabluda, S. G. Ovchinnikov, A. M. Potseluĭko, and S. A. Kharlamova, Fiz. Tverd. Tela (St. Petersburg) **47**, 474 (2005) [Phys. Solid State **47**, 489 (2005)].
24. Y. Tanabe and S. Sugano, J. Phys. Soc. Jpn. **9**, 753 (1951).
25. A. G. Gavrilyuk, I. A. Troyan, S. G. Ovchinnikov, et al., Zh. Éksp. Teor. Fiz. **126**, 650 (2004) [JETP **99**, 566 (2004)].
26. A. G. Gavriliuk, I. A. Trojan, R. Boehler, et al., Pis'ma Zh. Éksp. Teor. Fiz. **75**, 25 (2002) [JETP Lett. **75**, 23 (2002)].

Translated by A. Bagatur'yants